

Evolution of the Late Cretaceous crust in the equatorial region of the Northern Indian Ocean and its implication in understanding the plate kinematics

M. Desa^{1*}, M. V. Ramana¹, T. Ramprasad¹

¹*National Institute of Oceanography, Dona Paula, Goa, 403 004, India*

SUMMARY

Analysis of 3100 km of newly acquired marine magnetic data constrained by satellite and shipborne free air gravity anomalies in the corridor between the 86°E fracture zone and Ninetyeast Ridge, north of the equator reveals the evolutionary history of the Late Cretaceous crust characterised by anomaly 34 through 31 (83.5-68.7 Ma) under complex tectonic settings. Seafloor spreading model studies suggest that the crust, particularly between the chrons 33R and 33 (79.0 - 73.6 Ma) was formed with variable and slightly higher half-spreading rates (4.8 - 7.1 cm/yr) than the crust of similar age either in the regions west of 86°E fracture zone, east of the Ninetyeast Ridge or the Southern Crozet Basin. Further, the interpretation of magnetic anomalies suggests the presence of fossil spreading ridge segments and extra oceanic crust on the Indian plate that has been transferred from the Antarctica plate by discrete southward ridge jumps. These ridge jumps are caused by thermal instability of the spreading center as the Indian plate moved northward over the Kerguelen mantle plume. The present study indicates that the spreading ridge-plume interaction is the prime mechanism for these ridge jumps, which have occurred since 75.8 Ma. The newly identified magnetic anomalies 34 through 31 and the inferred ~N3°E trending fracture zones refined the plate reconstruction models for that period.

Key words: Gravity anomalies and Earth structure; Plate motions; Magnetic anomalies; Modeling and interpretation; Marine magnetics and palaeomagnetism; Oceanic transform and fracture zone processes; Crustal structure

Corresponding author: M. Desa, National Institute of Oceanography, Dona Paula, Goa India.
Tel. No.: +91 832 2450492; Fax. No.: +91 832 2450601; Email: mdesa@nio.org

1 INTRODUCTION

The Late Cretaceous-Cenozoic evolution of the Indian Ocean is well documented using seafloor spreading magnetic anomalies (e.g.: McKenzie & Sclater 1971; Sclater & Fisher 1974; Norton & Sclater 1979; Schlich 1982; Curray *et al.* 1982; Liu *et al.* 1983; Royer & Sandwell 1989; Duncan & Richards 1991). The Early Cretaceous evolution of the Indian Ocean is now well understood with the identification of Mesozoic magnetic anomalies M11 through M0 (~133-118 Ma) in the Bay of Bengal and its conjugate, the Enderby Basin, East Antarctica (Nogi *et al.* 1991, 1996; Ramana *et al.* 1994, 2001; Desa *et al.* 2006). Integrated geophysical and geological results under the constraints of Deep Sea Drilling [DSDP] and Ocean Drilling [ODP] Programs (Von der Borch, Sclater *et al.* 1974; Royer *et al.* 1989, 1991; Saunders *et al.* 1991; Duncan 1991) further enhanced our understanding of the plate kinematics in the Indian Ocean.

Evolution of the Indian Ocean can be documented in four main phases. During the first phase in the Early Cretaceous, India separated from the contiguous Antarctica-Australia (Powell *et al.* 1988; Royer *et al.* 1989; Royer & Coffin 1992; Ramana *et al.* 2001). During the second phase in the Middle Cretaceous, the first major plate reorganization took place and the direction of the Indian plate movement changed from northwest to north (Powell *et al.* 1988; Scotese *et al.* 1988; Royer & Sandwell 1989; Ramana *et al.* 1997). In the third phase i.e. from the Late Cretaceous to Middle Eocene, the Indian plate moved northwards with an average half-spreading rate of 12 cm/yr (Sclater & Fisher 1974). During the fourth phase, the second major plate reorganization due to the hard collision of the Indian plate with the Eurasian plate (Curray *et al.* 1982) resulted in a change in the Indian plate motion direction to northeast and the formation of present day Southeast Indian Ridge.

Major structural elements evolved in the Central Indian and Crozet Basins during the Late Cretaceous to Middle Eocene. The Afanasy Nikitin seamount chain on the Indian plate and the Conrad Rise on the Antarctica plate are the testimony for excessive volcanism on either side of the spreading ridge between India and Antarctica (McKenzie & Sclater 1971). The Ninetyeast Ridge, a trace of the Kerguelen mantle plume formed on the Indian plate during Middle Cretaceous to Late Eocene (Pierce 1978; Mahoney *et al.* 1983; Duncan 1991). The initiation of seafloor spreading between Australia and Antarctica, and the opening of the Wharton Basin took place during this period (Sclater & Fisher 1974; Crawford 1974; Fedorov *et al.* 1982; Liu *et al.* 1983). Though the Late Cretaceous to Early Tertiary evolutionary history of the Northern Indian Ocean covering the distal Bengal Fan is well established with the identification of magnetic

anomaly isochrons 34 through 31 (83.5 - 68.7 Ma) by earlier workers (McKenzie & Sclater 1971; Sclater & Fisher 1974; Norton & Sclater 1979; Schlich 1982; Royer *et al.* 1991), there still exists a large data gap in the region, particularly between 86°E fracture zone [FZ] and Ninetyeast Ridge, north of the equator. The magnetic anomalies west of the 86°E FZ are offset right-laterally by several N-S trending fracture zones, however, along the 86°E FZ, a left-lateral offset of about 900 km is reported by Sclater & Fisher (1974). East of the Ninetyeast Ridge, in the Wharton Basin, left-laterally offset magnetic anomalies (isochrons 32 and younger) are interpreted (Liu *et al.* 1983). Interpretation of magnetic data collected in the corridor 10 - 20°S latitudes and 80 - 100°E longitudes under the Trans Indian Ocean Geotraverse (TIOG) Programme brought out the spatial distribution of magnetic anomaly isochrons 32A through 19 and several fracture zones, in addition to a chain of fossil spreading ridge segments which ceased their activity around Early Eocene (Krishna *et al.* 1995). The data gap, west of Ninetyeast Ridge in the equatorial region of the Northern Indian Ocean, has limited our understanding about the evolution of oceanic crust adjacent to the Ninetyeast Ridge and thereby, the relative plate motions between India, Antarctica and Australia.

To establish the continuity of the structural fabric in the Northern Indian Ocean, particularly west and east of Ninetyeast Ridge, additional magnetic data has been acquired in the region north of the equator, between the 86°E FZ and the Ninetyeast Ridge. In this paper, we report the analysis of this data after its integration with the publicly available shipborne data (National Geophysical Data Center, NGDC, Colorado). We have identified magnetic anomaly isochrons 34 through 31 in this corridor, and proposed new oceanic fracture zones based on the observed offsets of successive isochrons. Further, we have inferred the presence of fossil spreading ridge [FSR] segments and about 62-85 km long extra crust between the chrons 33R and 31. These FSR segments are associated with magnetic anomalies symmetric about a central anomaly and a broad negative gravity field. Finally, we proposed refined plate reconstruction models for the Late Cretaceous period (chrons 34 and 31 time) using the newly identified magnetic anomalies, fracture zones and extra oceanic crust.

2 STUDY AREA

The principal study area (Block A), lies between 86° and 93°E longitudes and 1°S to 9°N latitudes in the equatorial region of the Northern Indian Ocean. This block includes the distal Bengal Fan, the northern part of the Ninetyeast Ridge and the northwestern part of the Wharton Basin (Fig.1). Late Cretaceous magnetic anomalies 34 through 31 were identified along the 86°E meridian

(McKenzie & Sclater 1971; Sclater & Fisher 1974; Royer *et al.* 1989). The oceanic crust of Wharton Basin, situated east of the Ninetyeast Ridge is characterized by magnetic anomaly sequence 32 and younger with age increasing towards north (Sclater & Fisher 1974; Liu *et al.* 1983). The corridor between the 86°E FZ and Ninetyeast Ridge lacks any magnetic anomaly identification.

Blocks B and C have been included in the present study to understand the evolutionary history of different provinces of similar age in the Indian Ocean (Fig. 1). Late Cretaceous magnetic anomalies 34 and younger, and their right lateral offset by several N-S trending fracture zones is well established in block B (e.g. McKenzie & Sclater 1971; Sclater & Fisher 1974; Royer *et al.* 1989; Schlich 1982). The N-S trending Afanasy Nikitin seamount chain lies in this region. Block C lies in the Southern Crozet Basin between Ob, Lena and Marion Dufresne seamount chain in the west and Kerguelen plateau in the east. Late Cretaceous to Tertiary magnetic anomalies (chrons 34 through 27) were identified by Schlich (1975, 1982) and Patriat (1987). The conjugate nature of the Northern Indian Ocean with the Southern Crozet Basin has been inferred from the plate reconstruction models for the Indian-Antarctic-Australian plates (Royer & Sandwell 1989). We have re-examined the existing data in these two blocks to strengthen our inferences on the evolution of the Late Cretaceous crust in Block A.

3 STRUCTURE AND TECTONIC SETTING

The seabed topography of the distal Bengal Fan in block A is smooth and depth to the seabed increases from 3400 to 4500 m towards south (Udintsev *et al.* 1975). The ocean floor is carpeted by <3 km thick sediments of Ganges and Brahmaputra rivers and pelagics (Curry 1994). The Ninetyeast Ridge, a submarine linear feature extends in an approximately north-south direction for more than 4,500 km between 31°S and 9°N latitudes and is surmised to extend several hundred kilometers farther north beneath the Bengal Fan sediments. The ridge has a relief of about 2000 m from the adjacent seafloor and about 300-500 m thick sediments are entrapped within its en-echelon segments (Sclater & Fisher 1974; Pierce 1978; Curry *et al.* 1982). It separates the Central Indian Basin from the Wharton Basin, and is bordered by a fracture zone consisting of a complex of ridges and graben-like troughs on its eastern side. Scientific drilling on the Ninetyeast Ridge during the Legs 22 and 26 of DSDP and Leg 121 of ODP (Luyendyk *et al.* 1973; Von der Borch, Sclater *et al.* 1974; Duncan 1991; Klootwijk *et al.* 1991) indicated that the ridge is volcanic in origin, and becomes progressively older to the north from the Oligocene to Late Cretaceous as do the magnetic anomaly isochrons observed to the west in the Central Indian Basin (McKenzie &

Sclater 1971). Further, the ridge was always attached to the Indian Plate, and formed in shallow water environment, sub-aerially exposed at times, and subsided along with the adjacent ocean floor according to the plate models of age-depth relationship (Von der Borch, Sclater *et al.* 1974; Stein & Stein 1992). The northern part of the ridge (north of 2°S) was emplaced as a result of intraplate volcanism on the Indian plate, and the ages along the ridge may not decrease monotonously from N-S because parts of the Antarctica plate were transferred to the Indian plate at different times (Royer *et al.* 1991). Further, the ridge is inferred to have evolved at a more southerly location and migrated north subsequently (Sclater & Fisher 1974). The Ninetyeast FZ which marks the thermal barrier limiting the extrusion of the plume in the Wharton Basin, kept progressing as the spreading center in the Wharton Basin migrated northward, while, the frequent ridge jumps kept the spreading center almost at a constant position west of the Ninetyeast Ridge (Royer & Sandwell 1989).

The Wharton Basin, situated east of the Ninetyeast Ridge, is associated with E-W trending left-laterally offset Tertiary magnetic anomaly sequence (Sclater & Fisher 1974). A fossil spreading ridge has been inferred based on the symmetric sets of magnetic anomalies 32 through 20 in this basin (Liu *et al.* 1983). This fossil ridge had been a part of the boundary between Indian and Australian plates, along which spreading activity ceased shortly after chron 20 (46 Ma), suggesting that the northwestern Wharton Basin was a part of the Indian plate from the Late Cretaceous to Eocene time (Liu *et al.* 1983).

The Central Indian Ocean Basin, including block B (Fig. 1) is dominated by east-west trending magnetic anomaly isochrons 34 through 22 offset right laterally by approximately N-S trending fracture zones, such as Indrani, Indira, 86°, etc. (McKenzie & Sclater 1971; Sclater & Fisher 1974; Krishna *et al.* 1995; Kamesh Raju & Ramprasad 1989). The magnetic anomalies are left-laterally offset by about 900 km along the 86°E FZ. At the axis of the Southeast Indian Ridge, the southward projection of this fracture zone offsets the ridge axis right-laterally by about 200 km. To make these two situations compatible, Sclater & Fisher (1974) suggested that: i) the ridge axis might have jumped at least eleven degrees towards south, and ii) the ridge jumps occurred any time since formation of anomaly 30.

Block C in the Southern Crozet Basin (Fig. 1) is associated with magnetic anomalies 34 and younger, with age decreasing towards north. These anomalies are right-laterally offset by several N28°E trending fracture zones. A major NNE-SSW trending fracture zone (Kerguelen FZ), west of Kerguelen Plateau, offsets the Late Cretaceous-Tertiary magnetic anomaly sequence left-laterally

by about 700 km (Schlich 1982). The Ob, Lena and Marion Dufresne seamount chain, aligns approximately in WNW-ESE direction, and rises to ~250 m from the surrounding water depth of about 4500 m. Goslin & Schlich (1982) suggested that the Afanasy Nikitin seamount chain in the Central Indian Basin and the Marion Dufresne seamount chain in the Crozet Basin were emplaced during an episode of anomalous volcanism in the vicinity of a spreading center.

4 DATA AND METHODOLOGY

About 3100 km of new magnetic, gravity and bathymetry data acquired on board ORV Sagar Kanya during the cruises SK82 and SK124 are used in the present study (Fig.1, Block A). The data comprises of three N-S profiles *Sk124-06*, *Sk124-08*, *Sk124-10* each about 500 km long that run roughly along 91, 89 and 88°E longitudes respectively; two short profiles *Sk124-11* and *Sk124-12* each about 200 km long, and a 1100 km long profile *Sk82-02* along 86.5°E longitude (Fig. 2A). In addition, about 5100 km of magnetic and bathymetry data retrieved from the archives of the NGDC, Colorado has been used in the present study to achieve good data coverage. Two N-S trending profiles (*Inmd7mv* and *Circ05ar* about 1200 km each from NGDC) are used in block B (Fig. 2B). About 5800 km of magnetic data has been used in the conjugate Southern Crozet Basin to support and strengthen our interpretation (Fig. 3). Profiles *Line1*, *Line2*, *Line4* and *Line5* were digitized with due care from the published magnetic anomaly maps (Sclater *et al.* 1996), while the profiles *C1705* and *Inmd05mv* were extracted from the NGDC. The processed magnetic data are plotted perpendicular to the cruise tracks and superimposed on the satellite derived free-air gravity mosaic (Sandwell & Smith 1997).

Late Cretaceous to Tertiary magnetic anomalies have been inferred in the Central Indian Ocean Basin, west of 86°E FZ (McKenzie & Sclater 1971; Sclater & Fisher 1974) and Wharton Basin, east of Ninetyeast Ridge (Liu *et al.* 1983). Similar magnetic anomalies are also reported in the Southern Crozet Basin (Schlich 1982; Patriat 1987; Sclater *et al.* 1996; Royer & Sandwell 1989) which is a conjugate of the Northern Indian Ocean. Since the study area (Block A) lies between the 86°E FZ and Ninetyeast Ridge, we presume the occurrence of similar magnetic anomalies in this corridor also. We therefore analyzed the newly acquired magnetic data in Block A using the seafloor spreading modeling technique and estimated the half-spreading rates. The magnetic profiles in Blocks B and C were also modeled.

5 RESULTS AND INTERPRETATION

The amplitude of the magnetic anomalies in the prime study area (Block A) varies between -600 and 400 nT (Fig. 2A). The pattern of the magnetic anomalies observed west of the 88°E longitude i.e., along the profiles *Sk82-02*, *Sk124-12*, and *Inmd6mv* is comparable with that observed along the profiles *Inmd7mv* in block B, and *lioecgs-b*, *84001211* and *Odp121jr* on the eastern side of the Ninetyeast Ridge (Fig. 2), and exhibit typical seafloor spreading magnetic anomaly characteristics. Though the magnetic anomaly pattern observed along the profiles *SK124-10*, *SK124-08* and *Dsdp22gc* is somewhat disturbed, the anomalies along the profiles can still be interpreted in terms of seafloor spreading. The profile *Sk124-06* traverses along the eastern flank of the Ninetyeast Ridge, and the magnetic signature along this profile seems to be influenced by the rugged topography.

5.1. Magnetic Model studies

The magnetic data in the Northern Indian Ocean and Southern Crozet Basin were modeled using the geomagnetic polarity time scale of Cande & Kent (1995). Synthetic seafloor spreading models have been generated by assuming uniformly magnetized blocks of oceanic crust with an average thickness of 500 m and a remanent magnetization of 0.01 A/m. The best-fit models are obtained with the paleo-spreading center located at 50°S latitude (Royer *et al.* 1991). Figure 4 depicts the synthetic seafloor spreading models and inter-profile anomaly correlation in the three blocks. In block A, anomalies 34 through 32A are confidently identified on profiles *Sk82-02* and *Inmd6mv*. Anomaly 33R is conspicuous on the profiles *Sk124-10* and *Sk124-08*. The profile *Sk124-10* intersects the profile *Inmd6mv* at the exact location where anomaly 33 has been identified. Thus the location of anomaly 33 along the profile *Sk124-10* is established and based on the correlation of anomalies, the anomalies 33 and 32A are identified on profile *Sk124-08*. The magnetic anomalies 34 through 31 are tentatively identified along the profile *Dsdp22gc* based on their correlation with the synthetic model.

Model studies facilitated in reconfirming the magnetic anomaly identifications 34 through 31 by earlier researchers in blocks B and C (Fig. 4). Further, our model studies suggest that the oceanic crust in the three blocks has evolved with variable half-spreading rates (HSR) (Fig. 5). The variation in spreading rates is seen between successive isochrons as well as within the same isochrons along adjacent profiles, more specifically between the anomaly isochrons 33R and 33 (e.g. profiles *Inmd7mv* and *Circ05ar*). The HSR between magnetic anomalies 34 and 33R varies

between 1.5 (*Sk82-02*) and 3.6 cm/yr (*Dsdp22gc*) in block A and is about 2.8 cm/yr in block B (*Inmd7mv* and *Circ05ar*). Between the anomalies 33R and 33, the HSR varies between 4.8 (*Sk82-02*) to 7.1 cm/yr (*Sk124-10*) in block A, while it is about 4.0 cm/yr along profile *Inmd7mv* and 7.0 cm/yr along profile *Circ05ar* on the Afanasy Nikitin Seamount chain in block B. The HSR stabilizes between 4 and 5 cm/yr for the younger anomalies 32 and 32A. However, along the profile *Dsdp22gc* between anomalies 32A and 31, the HSR is about 6 cm/yr. In block C, the crust between the chrons 34 to 33R has evolved with variable HSR of 4.0 to 4.7 cm/yr, while between the chrons 33R to 33, the HSR is between 4.5 and 5.3 cm/yr. It is conspicuous that the spreading rates between the chrons 34 and 33R are relatively high in this region when compared with the crust of similar age in block A. At the same time, the spreading rates are relatively low between the chrons 33R and 33 in block C when compared with that in block A (Fig. 5).

The inferred magnetic anomaly isochrons are plotted along the tracks to map the spatial distribution of the Late Cretaceous crust in block A (Fig. 6). Anomaly 34 lies around 5.7°N latitude and 86.5-86.9°E longitudes along the profiles *Sk82-02* and *Inmd6mv*, while it is located between 8.5-8.7°N latitudes and 90.5-91.15°E longitudes along the profiles *Dsdp22gc*, *Wi343811* and *Circ03*. The anomalies 33R through 31 are seen occurring with left lateral offsets and age decreasing towards south. Based on these offsets, we have inferred four new fracture zones FZ1 to FZ3 and FZ5 in addition to the previously identified 86°E, FZ4 (Ninetyeast FZ) and FZ6. Four new N28°E trending fracture zones (CFZ1 to CFZ4) are inferred east of the major Kerguelen fracture zone in the Southern Crozet Basin from the satellite derived gravity mosaic (Fig. 3).

5.2 Presence of Extra Crust

The high spreading rates particularly between chrons 33R and 33 (4.0 to 7.1 cm/yr) as seen in Figures 4 and 5, prompted us for critical evaluation of geophysical data in blocks A and B. Figure 7 depicts the stacking of magnetic anomalies with free-air gravity and bathymetry data along the N-S profiles in these blocks. The pattern of magnetic anomalies along those profiles with higher spreading rates (*Dsdp22gc*, *Sk124-08*, *Sk124-10* and *Circ05ar*) reveals symmetric disposition of magnetic anomalies about a central anomaly, and this portion of the crust is seen associated with a broad gravity low. This gravity low appears to be independent of topography except over a small pinnacle which causes a gravity high of about 10 mGals along the profile *Dsdp22gc*. Along the profile *Sk124-08*, the amplitude of the flanks of the broad gravity low is seen enhanced which may be due to the combined effect of the undulations in the crust and topography. The crust associated with the broad gravity low along the profile *Sk124-10* is devoid of any appreciable

variation in the topography. Along the profile *Circ05ar*, a prominent gravity low is observed despite lack of any bathymetric expression (Fig. 7a). We therefore conclude that this combination of broad gravity low and central magnetic anomaly represents a fossil spreading ridge (FSR). Another FSR segment is inferred along the profile *Dsdp22gc* at anomaly 32A (71.07 Ma) following the combination of symmetric magnetic anomalies, and a broad gravity low independent of bathymetry (Fig. 7b). The symmetric disposition of magnetic anomalies and associated broad gravity low facilitated in inferring the extent (62-85 km) of the extra crust. On plotting these FSR segments along with the extra crust on the track map (Fig. 6), we find that these FSR segments are offset left-laterally along with the adjacent crust.

6 DISCUSSION

Late Cretaceous magnetic anomaly sequence 34 through 31 and approximately N3°E trending oceanic fracture zones have been inferred in block A from the present study. The anomaly 34 identified on the Ninetyeast Ridge occurs south of the DSDP Site 217 (Fig. 6) where the age of the deepest sediment drilled is >80 Myr (Von der Borch, Sclater *et al.* 1974). Further, the identified magnetic anomaly 31 (68.7 Ma) lies north of the DSDP site 216, where the basement rocks yielded an age of about 66 Myr. Dating of the basement rocks at ODP site 758 yielded an age of about 81.8 Ma (Saunders *et al.* 1991; Duncan 1991), whereas Klootwijk *et al.* (1991) have inferred normal polarity (chron 33, 73.6 - 79.08 Ma) for these rocks. Our study indicates that the ODP site 758 lies on the inferred extra crust (Fig. 6), which has evolved during this normal polarity period. Royer and Sandwell (1989) place chron 34 (84 Ma) north of site 217 in their plate reconstructions, after incorporating two left lateral offsets with reference to its location at 86°E FZ. Further, in their reconstruction scenario, chron 31 is seen extending from the 86°E FZ upto the Ninetyeast FZ with a left lateral offset of about 2° at 88°E longitude. They also indicated the presence of a FSR in the vicinity of the ODP Site 758. Our study corroborated the presence of these inferred fracture zones, the western extent and left lateral disposition of the FSR and the spatial distribution of the magnetic anomalies (Fig. 6).

The synthetic seafloor spreading model (Fig. 4) depicts variable spreading rates for the anomaly sequence 34 through 31 in block A and this variation is observed not only for the different isochrons within the same profile, but also for the same isochron (particularly between 33R and 33) along different profiles (Fig. 5). Another important inference from the present study is the eastward increase in spreading rates between the isochrons 34 and 33, which is attributed to the readjustment of the spreading center while changing its orientation from NE-SW to E-W since

Middle Cretaceous. Average half-spreading rates of 5.7 and 6.0 cm/yr were estimated in the Central Indian Ocean and Wharton Basins respectively between the chrons 33 and 31 (Sclater & Fisher 1974; Liu *et al.* 1983), while about 5.4 cm/yr was estimated in the Southern Crozet Basin for the chrons 34 through 31 (Schlich 1982). Spreading rates inferred in the present study are low between the chrons 34 and 33R (1.5 - 3.6 cm/yr), and relatively high between 33R and 33 (4.0 - 7.1 cm/yr) in blocks A and B in the Northern Indian Ocean when compared with those estimated in block C (Fig. 5), suggesting the prevalence of asymmetric spreading from the beginning of Late Cretaceous.

Several major fracture zones have been identified distinctly in the Central Indian Ocean and Crozet Basins (Sclater & Fisher 1974; Norton & Sclater 1979; Schlich 1975, 1982; Kamesh Raju & Ramprasad 1989). Royer & Sandwell (1989) using plate reconstruction models established that the Kerguelen fracture zone and the 86°E FZ are complimentary to each other. Analysis of new magnetic data in block A resulted in the inference of new fracture zones in addition to the 86°E FZ and the Ninetyeast FZ. The 86°E FZ offsets the magnetic anomaly isochrons left-laterally by about 900 km. Further east, the magnetic anomalies are left-laterally offset by the newly identified fracture zones (Fig. 6). In the Southern Crozet Basin, west of Kerguelen fracture zone, the magnetic anomalies are right-laterally offset by three major fracture zones (Fig. 3). Along the Kerguelen fracture zone, a large left-lateral offset of about 700 km is conspicuous.

As mentioned in the results, the high spreading rates along some N-S profiles (*Sk124-10*, *Sk124-08* and *Dsdp22gc*) in block A are due to the presence of FSR segments and extra crust. Presence of these FSR segments suggests the readjustment of the spreading center in the form of southward ridge jumps since Late Cretaceous. The profile *Circ05ar* in block B is also characterized with high spreading rate and depicts the presence of FSR and 75 km long extra crust. FSRs have also been inferred between magnetic anomalies 30 and 26, west of the Ninetyeast Ridge (Royer *et al.* 1991). Interpretation of magnetic data in the region between 10-20°S and 80-100°E also revealed the presence of FSRs, which ceased their activity around anomaly 19 (Krishna *et al.* 1995). Presence of FSR in the distal Bengal Fan has been inferred using magnetic and gravity data within the Middle Cretaceous (Ramana *et al.* 1998). From the above observations, we believe that the spreading center between India and Antarctica was constantly undergoing readjustment since Middle Cretaceous to Early Eocene. The presence of the Kerguelen mantle plume in the vicinity of the spreading center might have caused these frequent readjustments (Duncan 1991; Saunders *et al.* 1991). According to Small (1995), the lithosphere above a mantle plume gets sufficiently weakened due to typical plume excess

temperatures to facilitate a ridge jump. As the India-Antarctica spreading center migrated northward (Muller *et al.* 1998), the Kerguelen mantle plume lagged behind on its southern flank and destabilized it. As a consequence, the spreading center jumped southward to this weak and hot zone leaving extra crust on the Indian plate.

The profiles *Circ05ar* and *Dsdp22gc* along the Afanasy Nikitin seamount chain and Ninetyeast Ridge, respectively, are located about 800 km apart, yet, exhibit similar magnetic anomaly signatures particularly between chrons 33R and 33 (Fig. 7). This observed similarity can be attributed to a common evolution mechanism triggered by the Kerguelen mantle plume, the influence of which can exceed 1000 km as suggested by Eldholm & Coffin (2000). Coffin *et al.* (2002) suggested either multiple plumes for the Kerguelen volcanics, or that the plume conduit was sheared by vigorous mantle flow into several diapirs. The present study endorses the influence of the Kerguelen mantle plume on the Ninetyeast Ridge, the region west of Ninetyeast Ridge and Afanasy Nikitin seamount chain as indicated above.

Bouligand *et al.* (2006) used sea surface magnetic profiles in different areas of the Indian and Pacific Oceans and observed tiny wiggles or micro-anomalies with polarity intervals less than 10 kyr within the major chrons during Late Cretaceous to Early Eocene. Further, they reported that in regions with high spreading rates, these wiggles were enhanced and better resolved. These tiny wiggles, referred as cryptochrons are attributed to short variations in the paleodipole field (Cande & Kent 1992). Bouligand *et al.* (2006) interpreted the profiles *Inmd7mv* (block B) and *Line2* (block C) along with other profiles and inferred 12 cryptochrons between the magnetic anomaly isochrons 33R and 33. Of the 12 cryptochrons, 'C' and 'B' representing 76.999 and 75.504 Ma respectively are the two prominent magnetic wiggles with diagnostic signatures. We have used their approach and geomagnetic field reversal data to generate the seafloor spreading model for the crust between the chrons 33R and 33 in the present study (Fig. 8). This exercise further supported our inferences on the presence of extra crust and FSR segments.

The profiles *Dsdp22gc*, *Sk124-08*, *Sk124-10* and *Circ05ar* with high spreading rates are seen associated with excess number of tiny wiggles, and exhibit good correspondence with the synthetic model after removal of these excess tiny wiggles (Fig. 8). These excess wiggles are the same that represent the inferred extra crust (Fig. 7). On the other hand, the profiles *Inmd7mv* and *Sk82-02* do not resolve the tiny wiggles distinctly due to lower spreading rates. A good correlation of the cryptochrons between all the profiles along with the model is discerned (Fig. 8). Subsequently, we estimated the half-spreading rates between the major chrons/cryptochrons

(Table 1). Detailed examination of the magnetic anomalies revealed the occurrence of a ridge jump around 75.8 Ma. This ridge jump is recorded along the profiles *Dsdp22gc* in block A and *Circ05ar* in block B, while it shows a time lag of about 0.278 and 0.789 Ma along the profiles *SK124-08* and *Sk124-10* respectively (Fig. 8). From the above inferences, we suggest that the region west of Ninetyeast Ridge and Afanasy Nikitin seamount chain, though under the influence of the Kerguelen mantle plume activity, retain the seafloor spreading magnetic anomaly signatures representing the geomagnetic field characteristics at the time of emplacement.

Muller *et al.* (1998, 2008) compiled crustal accretion rates for the world oceans and inferred that ridge-plume interaction is the main cause of spreading asymmetries even for large-plume distances. They estimated about 50-55% crustal accretion in the Southern Crozet Basin (block C) and about 45-70% and 45-50% in blocks A and B respectively. Thus, it is obvious that crustal accretion is predominant on the Antarctica plate and is relatively less on the Indian plate. An absolute northward ridge migration of about 5 cm/yr for the Indian plate between 83 and 67 Ma was also inferred (Muller *et al.* 1998). Our study indicates asymmetric crustal accretion as evidenced by varying spreading rates (Fig. 5) in the Northern Indian Ocean and Southern Crozet Basin.

6.1 Plate reconstructions

The present study facilitated in identification of new magnetic anomalies, fracture zones and extra crust in block A which are used as constraints for generating plate reconstruction models for the chrons 34 and 31 (Fig. 9) using the published/modified rotation pole parameters as shown in Table 2. The reconstructions are well constrained by several identifications of chrons 34 and 31 in the Central Indian and Crozet Basins. However, due to lack of these anomaly identifications in the Wharton Basin, we assumed constant anomaly offsets along the fracture zones and symmetric spreading in space and time, to calculate the older anomaly locations from the few younger picks on either side of the Wharton fossil ridge. Initially, we used the pole parameters of Royer & Sandwell (1989) for the reconstructions, but we noticed small discrepancies in the fit of the conjugate fracture zones and location of magnetic anomalies. Accordingly, we readjusted the pole parameters in order to narrow down these discrepancies and generated refined plate reconstruction models for chrons 34 and 31. Any remaining small-scale discrepancy has been attributed to asymmetric spreading as indicated by the variable half-spreading rates (Fig. 5).

Chron 34 reconstruction: Several identifications of chron 34 west of the major Kerguelen FZ (McKenzie & Sclater 1971; Sclater & Fisher 1974) and few picks east of this fracture zone from the present study depict a good fit of this reconstruction. The inferred fracture zones FZ1 and FZ3 in the Northern Indian Ocean (block A) match well with CFZ2 and CFZ3 respectively from the Southern Crozet Basin (Fig. 9a). This model also depicts an excellent match of the anomaly 34 between Australia and Antarctica, and a triple junction at the western edge of the combined Kerguelen Plateau and Broken Ridge as shown by Royer & Sandwell (1989). Very slow transform motion is inferred at the western end of the Australia-Antarctica plate boundary through the Kerguelen Plateau. Royer & Sandwell (1989) inferred relative strike slip motion between the Central and Southern Kerguelen Plateau along the N-S trending 77°E graben. We have incorporated this motion in our reconstruction by rotating the Central Kerguelen Plateau with respect to the Southern Kerguelen Plateau using the pole parameters as shown in Table 2, which reduced the overlap considerably between the Kerguelen Plateau and Broken Ridge (Fig. 9a). The Kerguelen mantle plume lies around the western edge of the Central Kerguelen Plateau where the formation of the Ninetyeast Ridge just initiated.

Chron 31 reconstruction: The new constraints in block A yielded a good fit for the chron 31 and excellent correspondence of the fracture zones (Fig. 9b). Relative strike slip motion of ~60 km between Central and Southern Kerguelen Plateau (Table 2) continued from chron 34 to 31 along the 77°E graben. We have incorporated the crustal accretion rates of Muller *et al.* (2008) for the crust generated between chrons 34 and 31. Excess accretion (50-55%) on the Antarctica plate is reported west of CFZ2 (Fig.9b), while, east of FZ1 (complement of CFZ2), the accretion asymmetry reverses with more than 55% on the Indian plate. The extra crust inferred in our study in the corridor between the 86°E FZ and Ninetyeast Ridge is responsible for the excess crustal accretion. Thus, the observed crustal accretion asymmetry on the Indian and Antarctica plates is due to the combined effect of ridge jumps and differential spreading rates. The profiles *Inmd7mv* and *Circ05ar* from block B projected in this reconstruction are conjugate to the profiles *Line2* and *C1705* of block C respectively (Fig. 9b). These two conjugate pairs were studied further to validate our interpretation in on the occurrence of ridge jumps.

The wiggle to wiggle correlation of the magnetic anomalies between the conjugate lines *Inmd7mv* and *Line2* is shown in figure 10a. There is an excellent correlation between the major anomalies and wiggles with the respective models thereby confirming the ages. The spreading rates are higher along profile *Line2* as compared to profile *Inmd7mv* suggesting excess crustal accretion on the Antarctica plate as evidenced in Figure 9b. Profile *Circ05ar* traversing the

Afanasy Nikitin seamount chain is modeled after removal of the inferred extra crust and compared with its conjugate profile *C1705* (Fig. 10b). Since these profiles *Circ05ar* and *C1705* are situated in northern and southern hemispheres respectively, we have deskewed the profile *C1705* by 90° and made a wiggle to wiggle comparison. On adding the extra crust inferred on the profile *Circ05ar*, at its appropriate location on the deskewed profile *C1705*, good correlation of the major chrons, wiggles and cryptochrons is achieved (Fig. 10b). Further, the unequal lengths of the elevated topography along these two profiles endorse our inference about the presence of extra crust along the profile *Circ05ar*.

6.2 Tectonic implication

The presence of Late Cretaceous oceanic crust of 83.5 to 68.7 Myr age (magnetic anomalies 34 through 31) in the corridor between the 86°E FZ and Ninetyeast Ridge, and the occurrence of similar age crust west of 86°E FZ and east of Ninetyeast Ridge in the Northwestern Wharton Basin implies that this corridor evolved contemporaneously with the adjacent ocean floor (Fig. 6). Southward ridge jumps due to thermal instability of the spreading center occurred in this corridor since 75.8 Ma and captured about 62-85 km long crust from the Antarctica plate. A similar southward ridge jump seems to have occurred on the Afanasy Nikitin Seamount chain around the same time. These ridge jumps kept the spreading center nearly at the same position in the vicinity of the Kerguelen mantle plume, west of the Ninetyeast Ridge/FZ as the Indian plate moved northward. Excess crustal accretion on the Antarctica plate due to asymmetric spreading prevailed during this period. However, frequent southward ridge jumps and higher spreading rates resulted in excess crustal accretion (upto 70%) on the Indian plate in the corridor between the 86°E FZ and Ninetyeast Ridge.

7 CONCLUSIONS

Analysis of marine magnetic data in the corridor between the 86°E FZ and Ninetyeast Ridge north of equator reveals that the Late Cretaceous crust of 83.5 – 68.7 Myr age has evolved with variable spreading rates. Model studies suggest that the crust particularly between the magnetic anomaly isochrons 33R and 33 has formed with relatively higher half-spreading rates of 4.8 - 7.1 cm/yr, and is associated with FSR segments and about 62 - 85 km extra crust. This extra crust is left-laterally offset by N3°E trending fracture zones along with the adjacent oceanic crust. A FSR and about 75 km extra crust inferred along the Afanasy Nikitin seamount chain is attributed to a ridge jump that occurred around 75.8 Ma. The presence of extra crust

and similar magnetic anomaly signatures on the Afanasy Nikitin seamount chain and Ninetyeast Ridge particularly between the chrons 33R and 33 suggest a common evolution mechanism. The inferred extra crust has been captured from the Antarctica plate by southward ridge jumps as the spreading center tried to remain in the vicinity of Kerguelen mantle plume during the northward motion of the Indian plate. Our study further suggests that ridge-plume interaction manifested in the form of southward ridge jumps occurred as early as 75.8 Ma and up to 5.4°N latitude.

Refined plate reconstruction models under the constraints of newly identified magnetic anomalies and fracture zones accounted for the presence of extra crust and FSR segments in the Northern Indian Ocean. Though excess crustal accretion due to asymmetric spreading is reported on the Antarctica plate between the chrons 34 and 31, the inferred extra crust and higher spreading rates are responsible for the excess crustal accretion on the Indian plate in the corridor between the 86°E FZ and Ninetyeast Ridge.

ACKNOWLEDGEMENTS

We sincerely thank the anonymous reviewers for their constructive comments which enhanced the quality of the manuscript. We would like to thank Director, NIO for granting necessary permission. The officers, crew, scientific and supporting staff who participated in the ORV Sagar Kanya cruises SK82 and SK124 are duly acknowledged. GMT software (Wessel & Smith 1998) was used to generate the maps in this paper. This is NIO contribution no 4494.

REFERENCES

- Bouligand, C., Dyment, J., Gallet, Y. & Hulot, G., 2006. Geomagnetic field variations between chrons 33r and 19r (83-41 Ma) from sea-surface magnetic anomaly profiles, *Earth Planet. Sci. Lett.*, **250**, 541-560.
- Cande, S.C. & Kent, D. V., 1992. Ultrahigh resolution marine magnetic anomaly profiles: a record of continuous paleointensity variations? *J. Geophys. Res.*, **97**, 15075-15083.
- Cande, S. C. & Kent, D. V., 1995. Revised calibration of the geomagnetic polarity time scale for the Late Cretaceous and Cenozoic, *J. Geophys. Res.*, **100**, 6093 - 6095.
- Coffin, M. F., Pringle, M. S., Duncan, R. A., Gladchenko, T. P., Storey, M., Muller, R. D. & Gahagan, L. A., 2002. Kerguelen hotspot magma output since 130 Ma, *J. Petrology*, **43**, 1121 - 1139.
- Crawford, A. R., 1974. Indo-Antarctica, Gondwanaland, and the distortion of a granulite belt, *Tectonophysics*, **22**, 141-157.
- Curry, J. R., 1994. Sediment volume and mass beneath the Bay of Bengal, *Earth Planet. Sci. Lett.*, **125**, 371-383.
- Curry, J. R., Emmel, F. J., Moore, D. G. & Raitt, R. W., 1982. Structure, tectonics and geological history of the Northeastern Indian Ocean, in *The Ocean Basins and Margins*, eds Nairn, A. E. & Stehli, F. G., Plenum, New York, **6**, 399-450.
- Desa, M., Ramana, M. V. & Ramprasad, T., 2006. Seafloor spreading magnetic anomalies south off Sri Lanka, *Mar. Geol.*, **229**, 227 - 240.
- Duncan, R. A., 1991. Age distribution of volcanism along aseismic ridges in the eastern Indian Ocean, in *Proc. ODP, Sci. Results*, **121**, 507-517, eds Weissel, J. K., Peirce, J. *et al.*, Ocean Drilling Program, College Station, TX.
- Duncan, R. A. & Richards, M. A., 1991. Hotspots, mantle plumes, flood basalts and true polar wander, *Rev. Geophys.*, **29**, 31 - 50.
- Eldholm, O. & Coffin, M. F., 2000. Large igneous provinces and plate tectonics, in *The History and Dynamics of Global Plate Motions*, **121**, 309-326, eds Richards, M. A., Gordon, R. G. & van der Hilst, R. D., *Geophys. Monograph*, American Geophysical Union, Washington.
- Fedorov, L. V., Grikurov, G. E., Kurinin, R. G. & Masolov, V. N., 1982. Crustal structure of the Lambert Glacier Area from geophysical data, in *Antarctica Geoscience*, eds Craddock, C., Loveless, J. K., Vierima, T. L. & Crawford, K., *University of Wisconsin Press, Madison, WI*, 931-936.
- Goslin, J. & Schlich, R., 1982. Structural limits of the South Crozet Basin – Relations to Enderby Basin and the Kerguelen-Heard Plateau, in *Antarctica Geoscience*, eds Craddock, C., Loveless, J. K., Vierima, T. L. & Crawford, K., *University of Wisconsin Press, Madison, WI*, 79-85.

- Kamesh Raju, K. A. & Ramprasad, T. 1989. Magnetic lineations in the Central Indian Basin for the period A24-A21: A study in relation to the Indian Ocean Triple Junction trace, *Earth Planet. Sci. Lett.*, **95**, 395 - 402.
- Klootwijk, C. T., Gee, J. S., Pierce, J. W. & Smith, G. M., 1991. Constraints on the India – Asia convergence: paleomagnetic results from Ninetyeast Ridge, in *Proc. ODP, Sci. Results*, **121**, 777-882, eds Weissel, J. K., Peirce, J. *et al.*, Ocean Drilling Program, College Station, TX.
- Krishna, K. S., Gopala Rao, D., Ramana, M. V., Subrahmanyam, V., Sarma, K.V.L.N.S., Pilipenko, A. I., Shcherbakov, V. S. & Murthy, I. V. R., 1995. Tectonic model for the evolution of oceanic crust in the northeastern Indian Ocean from the Late Cretaceous to the Early Tertiary, *J. Geophys. Res.*, **100**, 20011 - 20024.
- Liu, C. S., Curray, J. R. & McDonald, J. M., 1983. New constraints on the tectonic evolution of eastern Indian Ocean, *Earth Planet. Sci. Lett.*, **65**, 331 - 342.
- Luyendyk, B. P. *et al.*, 1973. Leg 26, Deep Sea Drilling Project: Across the Southern Indian Ocean aboard Glomar Challenger, *Geotimes*, **18**, 16-19.
- Mahoney, J. J., Macdougall, J. D., Lugmair, G. W. & Gopalan, K., 1983. Kergulen hotspot source for Rajmahal Traps and Ninetyeast Ridge? *Nature*, **303**, 385 - 389.
- McKenzie, D. & Sclater, J. G., 1971. The evolution of the Indian Ocean since the Late Cretaceous, *Geophys. J. R. Astr. Soc.*, **25**, 437 - 528.
- Muller, R. D., Roest, W. R. & Royer, J-Y., 1998. Asymmetric sea-floor spreading caused by ridge-plume interactions, *Nature*, **396**, 455 - 459.
- Muller, R. D., Sdrolias, M., Gaina, C. & Roest, W. R., 2008. Age, spreading rates, and spreading asymmetry of the world's ocean crust, *Geochem. Geophys. Geosyst.*, **9**, Q04006, doi:10.1029/2007GC001743.
- Nogi, Y., Seama, N., Isezaki, N., Hayashi, T., Funaki, M. & Kaminuma, K., 1991. Geomagnetic anomaly lineations and fracture zones in the basin west of Kerguelen Plateau, *EOS Trans. Am. Geophys. Un.*, **72**, 445.
- Nogi, Y., Seama, N., Isezaki, N. & Fukuda, Y., 1996. Magnetic anomaly lineation and fracture zone formations deduced from vector data of the geomagnetic anomaly field in the west Enderby Basin adjacent to the Weddell Sea, in *Weddell Sea Tectonics and Gondwana Breakup*, **108**, 265 – 273 eds Storey, B. C., King, E. C. & Livermore, R. A., *Geol. Soc. Spec. Publ*, The Geological Society Publishing House, Bath.
- Norton, I. O. & Sclater, J. G., 1979. A model for the evolution of the Indian Ocean and the break up of Gondwanaland, *J. Geophys. Res.*, **84**, 6803 - 6830.
- Patriat, P., 1987. Reconstitution de l'évolution du système de dorsales de l'Océan Indien par les méthodes de la cinématique des plaques, Territoires des Terres Australes et Antarctique Françaises, Paris.

- Peirce, J. W., 1978. The northward motion of Indian since the Late Cretaceous, *Geophysics Jour. R. Astr. Soc.*, **52**, 277 – 311.
- Powell, C. M., Roots, S. R. & Veevers, J. J., 1988. Pre-breakup continental extension in East Gondwanaland and the early opening of the eastern Indian Ocean, *Tectonophysics*, **155**, 261-283.
- Ramana, M. V., Nair, R. R., Sarma, K. V. L. N. S., Ramprasad, T., Krishna, K. S., Subrahmanyam, V., D'Cruz, M., Subrahmanyam, C., Paul, J., Subrahmanyam, A. S. & Chandrasekhar, D. V., 1994. Mesozoic anomalies in the Bay of Bengal, *Earth Planet. Sci. Lett.*, **121**, 469 - 475.
- Ramana, M. V., Subrahmanyam, V., Sarma, K.V.L.N.S., Desa, M., Malleswara Rao, M. M. & Subrahmanyam, C., 1997. Record of the Cretaceous Magnetic Quiet Zone: A precursor to the understanding of the evolutionary history of the Bay of Bengal, *Curr. Sci.*, **72**, 669 - 673.
- Ramana, M. V., Subrahmanyam, V., Sarma, K. V. L. N. S., Desa, M. & Ramprasad, T., 1998. Boundary of magnetic anomaly isochron A34 (~84 Ma) in the southern Bay of Bengal. *35th Annual Convention and Meeting on Continental Margins of India – Evolution, Processes and Potentials*, Abstract Volume, p. 12, Indian Geophysical Union, Hyderabad.
- Ramana, M. V., Ramprasad, T. & Desa, M., 2001. Seafloor spreading magnetic anomalies in the Enderby basin, East Antarctica, *Earth Planet. Sci. Lett.*, **191**, 241-255.
- Royer, J-Y. & Sandwell, D. T., 1989. Evolution of the eastern Indian Ocean since the Late Cretaceous: Constraints from GEOSAT altimetry, *J. Geophys. Res.*, **94**, 13755 -13782.
- Royer, J-Y., Sclater, J. G. & Sandwell, D. T., 1989. A preliminary tectonic fabric chart of the Indian Ocean, *Proc. Ind. Acad. Sci., Earth Planet. Sci.*, **98**, 7 - 24.
- Royer, J-Y., Peirce, J. W. & Weissel, J. K., 1991. Tectonic constraints on the hot-spot formation of Ninetyeast Ridge, in *Proc. ODP, Sci. Results*, **121**, 763 – 776, eds Weissel, J. K., Peirce, J., *et al.*, Ocean Drilling Program, College Station, TX.
- Royer, J. Y. & Coffin, M. F., 1992. Jurassic to Eocene plate tectonic reconstructions in the Kerguelen plateau region, in *Proc. ODP, Sci. Results*, **120**, 917 – 928, eds Wise, Jr. S. W., Schlich, R., *et al.*, Ocean Drilling Program, College Station, TX.
- Sandwell, D. T. & Smith, W. H. F., 1997. Marine gravity anomaly from GEOSAT and ERS-1 satellite altimetry, *J. Geophys. Res.*, **102**, 10039-10054.
- Saunders, A. D., Storey, M., Gibson, I. L., Leat, P., Hergt, J. & Thompson, R. N., 1991. Chemical and isotopic constraints on the origin of basalts from Ninetyeast Ridge, Indian Ocean: results from DSDP Legs 22 and 26 and ODP Leg 121, in *Proc. ODP, Sci. Results*, **121**, 559 – 590, eds Weissel, J. K., Peirce, J. *et al.*, Ocean Drilling Program, College Station, TX.
- Schlich, R., 1975. Structure et age de l'ocean Indien occidental, *Mem. Hors. Ser. Soc. Geol. Fr*, **6**, 103 pp.

- Schlich, R., 1982. The Indian Ocean: aseismic ridges, spreading centers and ocean basins, in *The Ocean Basins and Margins*, eds Nairn, A. E., & Stehli, F. G., Plenum, New York, **6**, 51-147.
- Sclater, J. G. & Fisher, R. L., 1974. Evolution of the east Central Indian Ocean with emphasis on the tectonic setting of the Ninetyeast Ridge, *Geol. Soc. Amer. Bull.*, **85**, 683 - 702.
- Sclater, J. G., Munsch, M. *et al.*, 1996. Geophysical synthesis of the Indian/Southern Oceans: Part 1, The southwest Indian Ocean, SIO Ref. Series No 97-06, 45 pp, University of California, San Diego, CA.
- Scotese, C. R., Gahagan, L. M. & Larson, R. L., 1988. Plate tectonic reconstructions of the Cretaceous and Cenozoic ocean basins, *Tectonophysics*, **155**, 27 - 48.
- Small, C., 1995. Observations of ridge-hotspot interactions in the Southern Ocean, *J. Geophys. Res.*, **100**, 17931-17946.
- Stein, C. A. & Stein, S. 1992. A model for the global variation in oceanic depth and heat flow with lithospheric age, *Nature*, **359**, 123-129.
- Udintsev, G. B., Fisher, R. L., Kanaev, V. F., Laughton, A. S., Simpson, E. S. W. & Zhiv, D. I., 1975. *Geological-Geophysical Atlas of the Indian Ocean*, Academy of Sciences of the U.S.S.R., Moscow, 151 pp.
- Von der Borch, C. C., Sclater, J. G. *et al.*, 1974. *Initial Reports of the Deep Sea Drilling Project*, **22**, Washington U. S. Govt. Printing Office, 890 pp.
- Wessel, P. & Smith, W. H. F., 1998. New improved version of Generic Mapping Tools released, *EOS Trans. Am. Geophys. Un.*, **79**, 579.

FIGURE CAPTIONS

Fig. 1. Generalized tectonic map of the Indian Ocean (Royer *et al.* 1989). The blocks A, B and C represent the study areas. Fracture zones (dashed lines) and magnetic lineations (solid red lines, a few of which are labeled with magnetic anomaly numbers) are from earlier works (Royer *et al.* 1989; Ramana *et al.* 2001; Desa *et al.* 2006). DSDP and ODP sites are indicated as small, open circles. Thick continuous lines represent fossil spreading ridges (Royer *et al.* 1989; Krishna *et al.* 1995). Blue enclosures represent large igneous provinces. NER - Ninetyeast Ridge; CLR -Chagos-Laccadive Ridge; SL-Sri Lanka; CB - Crozet Basin; EB - Elan Bank; ST - Sunda Trench; 85ER - 85°E Ridge; OB – Ob, Lena & Marion Dufresne seamount chain; BR – Broken Ridge; KP – Kerguelen Plateau; MDG – Madagascar; CR-Comorin Ridge; CBR – Carlsberg Ridge; CIR – Central Indian Ridge; SWIR – Southwest Indian Ridge; SEIR – Southeast Indian Ridge; WB – Wharton Basin; KFZ – Kerguelen Fracture Zone; KI – Kerguelen Island; DBF – Distal Bengal Fan; 86FZ – 86° FZ; ANS – Afanasy Nikitin seamount chain.

Fig. 2. Residual magnetic anomalies plotted perpendicular to the cruise tracks superimposed on the satellite derived free-air gravity mosaic (Sandwell & Smith 1997) for the blocks A and B. Positive magnetic anomalies are shaded white and projected towards right. Previously identified magnetic anomalies and fracture zones are indicated as continuous and dashed lines respectively (Royer *et al.* 1991; Desa *et al.* 2006). Magnetic anomaly isochrons are indicated with numbers. Drill sites that did not reach basement are indicated as red solid circles, while those that recovered basement rocks are indicated as black solid circles.

Fig. 3. Residual magnetic anomalies plotted perpendicular to the cruise tracks superimposed on the satellite derived free-air gravity mosaic (Sandwell & Smith 1997) for the Southern Crozet Basin (block C). Positive magnetic anomalies are shaded white and projected towards left. Fracture zones and magnetic lineations are indicated as dashed lines and continuous lines respectively (Schlich 1975, 1982). Magnetic anomaly isochrons are indicated with numbers. Drill sites that did not reach basement are indicated as red solid circles, while those that recovered basement rocks are indicated as black solid circles. Age in Myr of the basement rocks is indicated in brackets. CFZ1 to CFZ4 are the newly inferred fracture zones. CKP – Central Kerguelen Plateau; NKP – Northern Kerguelen Plateau; KFZ - Kerguelen Fracture zone; KI – Kerguelen Island.

Fig. 4. Magnetic profiles plotted along with their respective synthetic seafloor spreading models in the blocks A, B and C. The geomagnetic polarity time scale of Cande & Kent (1995) is

used to constrain the anomalies 34 through 31. The models were computed for the oceanic crust generated at a paleolatitude of 50°S with a thickness of the magnetized layer of 500 m and a remanent magnetization of 0.01 A/m. FZ indicates fracture zone. The locations of the profiles are shown in figures 2 and 3. Half-spreading rates are in cm/yr.

Fig. 5. Half-spreading rates calculated for individual profiles plotted against time (67 - 85 Ma) for the Late Cretaceous anomalies in the northern Indian Ocean (blocks A and B) and Southern Crozet Basin (block C). Higher spreading rates between chrons 33R and 33, and lower spreading rates between chrons 34 and 33R are conspicuous in the Northern Indian Ocean.

Fig. 6. Map depicting the newly interpreted and earlier identified (Liu *et al.* 1983; Royer *et al.* 1991) magnetic anomalies (continuous lines) in block A. Fracture zones, both old (FZ4 and FZ6) and new (FZ1, FZ2, FZ3 and FZ5) are indicated as dashed lines. Continuous blue line depicts the 3000m depth contour. The new anomaly identifications are based on the synthetic model shown in Fig. 4. Drill sites that did not reach basement are indicated as red solid circles, while those that recovered basement rocks are indicated as black solid circles. Age in Myr of the oldest sediments/basement rocks is indicated in brackets. Thick black line represents the fossil spreading ridge segments, while light shaded box represents the inferred extra crust.

Fig. 7. Composite plot of satellite derived/shipborne free-air gravity, magnetics and bathymetry along the N-S profiles in blocks A and B stacked with respect to: a) anomalies 33R through 33, and b) anomalies 33 through 31. Symmetrical magnetic anomalies about a central anomaly are associated with a gravity low (GL). The central magnetic anomaly corresponds to the inferred fossil spreading ridge (FSR) segment (thick vertical block). Symmetrical magnetic anomalies are shown in gray shade box, and the corresponding anomalies on either side of the central anomaly are shown with solid circle and star. EC represents the extra crust captured from the Antarctica plate.

Fig. 8. Magnetic anomalies along the N-S profiles in blocks A and B stacked with respect to chrons 33R through 33. The extra crust as indicated in figure 7 has been plotted in a reverse direction (blue outline) to better appreciate the symmetry. Correlation of major chrons and cryptochrons/wiggles between the profiles is shown by red dashed lines. The ages are constrained by the synthetic seafloor spreading model generated for profile *Circ05ar* using the same parameters as in figure 4 with additional geomagnetic polarity reversal information of Bouligand *et al.* (2006). The wiggles 'C' and 'B' represent 76.999 and 75.504 Ma

cryptochrons respectively. The cryptochron of 74.662 Ma is designated with 'A' in the present study. Half-spreading rates are in cm/yr, while the ages for the wiggles are in Myr.

Fig. 9. Plate reconstruction models depicting the palaeo positions of India/Antarctica/Australia for: a) chron 34, and b) chron 31. The reconstructions are made using the rotation parameters as indicated in Table 2. Fracture zones and magnetic anomalies are indicated as dashed and continuous lines respectively. Palaeo positions of DSDP and ODP sites are shown. The star represents the location of the Kerguelen mantle plume. The probable western extent of the Australia-Antarctica spreading center through the 77°E graben (thick line) is indicated as dashed line. Early Cretaceous magnetic anomalies and fracture zones (Ramana *et al.* 2001; Desa *et al.* 2006) are shown in the Bay of Bengal, Northeastern Indian Ocean and Enderby Basin, East Antarctica. KFZ – Kerguelen Fracture Zone. The conjugate profiles used for detailed study are indicated as thick black lines. Extra crust inferred in the present study is shown as black patches. Crustal accretion asymmetry as inferred by Muller *et al.* (2008) is shown in color code.

Fig. 10. (A) Magnetic anomalies along the conjugate profiles *Line2* and *Inmd7mv* with their synthetic models. Excellent correlation between the magnetic anomalies is depicted. Higher spreading rates (cm/yr) prevail along *Line2* as compared to *Inmd7mv*.

(B) Magnetic anomalies and bathymetry (thick blue) along the conjugate profiles *C1705* and *Circ05ar* (inferred extra crust plotted reversed) with their synthetic models. The variable extent of elevated topography along these profiles indicates the presence/absence of crust. The deskewed profile *C1705* is plotted along with the extra crust inferred on profile *Circ05ar* to validate our inference of ridge jump. A good correlation is now seen between the wiggles/cryptochrons on the deskewed profile *C1705* and *Circ05ar* (dashed lines). Half-spreading rates are indicated in cm/yr, while the ages corresponding to the wiggles are in Myr.

LIST OF TABLES

Table 1: Half-spreading rates (HSR, cm/yr) calculated for different chrons/cryptochrons for the N-S profiles in block A and the conjugate profiles in blocks B and C. Before estimating the HSR, the inferred extra crust is removed along the profiles *Dsdp22gc*, *SK124-08*, *Sk124-10* and *Circ05ar*, while along the profile *C1705*, the missing crust is added.

Table 2: Finite rotation parameters used for generating plate reconstructions at chrons 34 and 31. Antarctica is kept in its present day position. Angles are positive counterclockwise.

Table 1:

Profile	34-33R	33R-C	C-B	B-A	A-33	33-32A	32A-31
	(83.5- 79.08)	(79.08- 77)	(77- 75.5)	(75.5- 74.6)	(74.6- 73.6)	(73.6- 71.07)	(71.07- 68.7)
Block A							
Sk82-02	1.5	3.5	5.6	5.4	5.4	4.6	4.6
Sk124-10	-	3.7	6.9	7.7	7.9	-	-
Sk124-08	-	4.0	6.2	7.0	6.0	3.9	-
Dsdp22gc	3.6	4.2	5.6	5.0	5.0	4.4	3.5
Block B							
Inmd7mv	2.9	3.7	3.7	4.6	4.6	4.2	4.3
Circ05ar	2.7	3.3	6.2	7.8	7.8	4.8	4.8
Block C							
Line2	4.0	4.6	4.8	4.4	4.4	4.6	-
C1705	-	4.2	6.3	8.5	8.5	5.7	-

Table 2:

Chron	Age (Ma)	Latitude (+°N)	Longitude (+°E)	Angle (°)	Reference
India relative to Antarctica					
34	83.5	8.8	11.2	-64.5	Modified from Royer & Sandwell (1989)
31	68.7	8.8	13.8	-52.5	Modified from Royer & Sandwell (1989)
Australia relative to Antarctica					
34	83.5	4.9	35.8	-27.81	Modified from Royer & Sandwell (1989)
31	68.7	8.7	33.2	-25.83	Royer & Sandwell (1989)
Central Kerguelen Plateau relative to Southern Kerguelen Plateau					
34	83.5	-54.4	50.4	-5.41	Royer & Sandwell (1989)
31	68.7	-55.0	38.1	-3.16	Royer & Sandwell (1989)

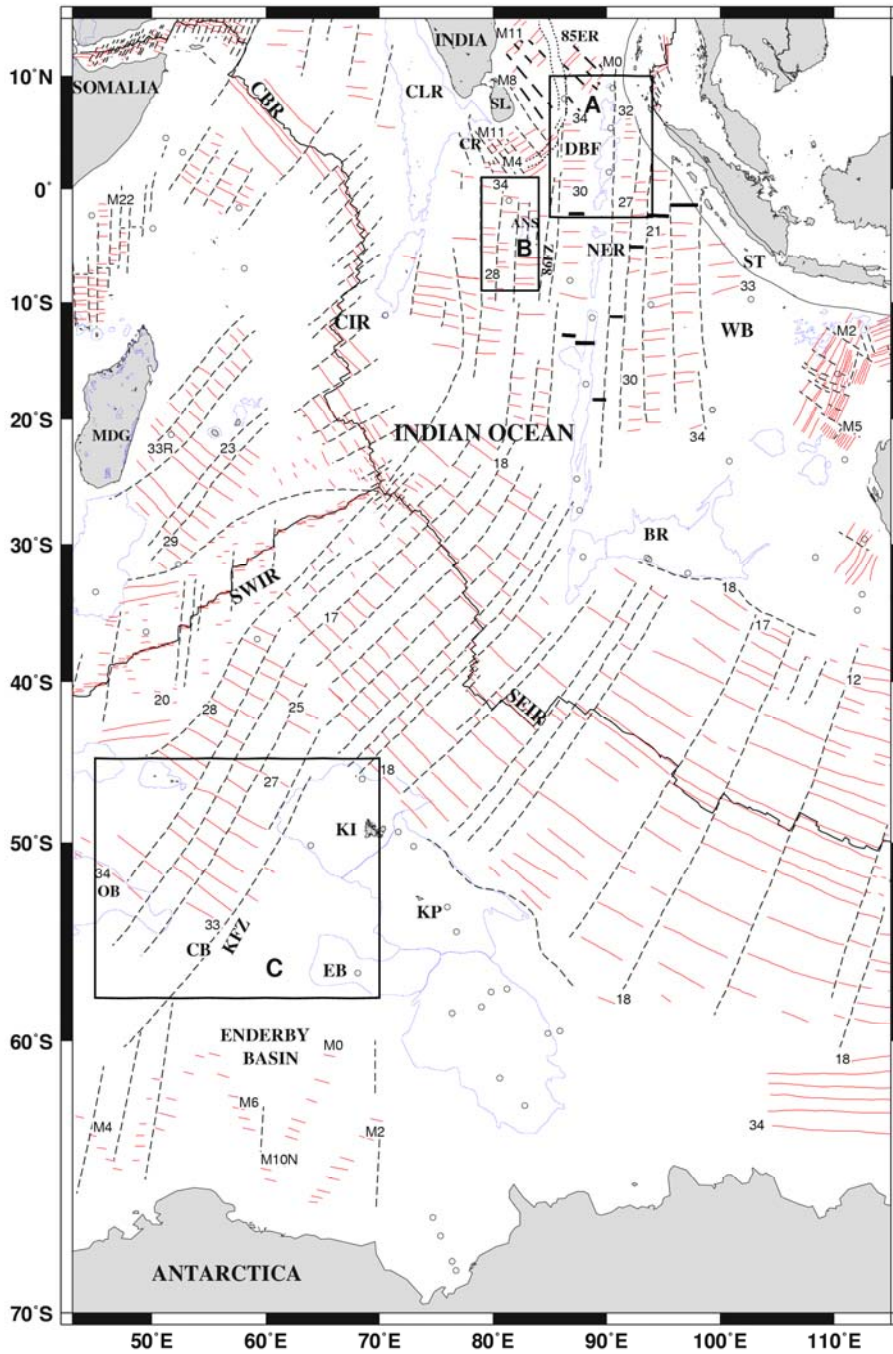


Fig. 1
Desa et al.

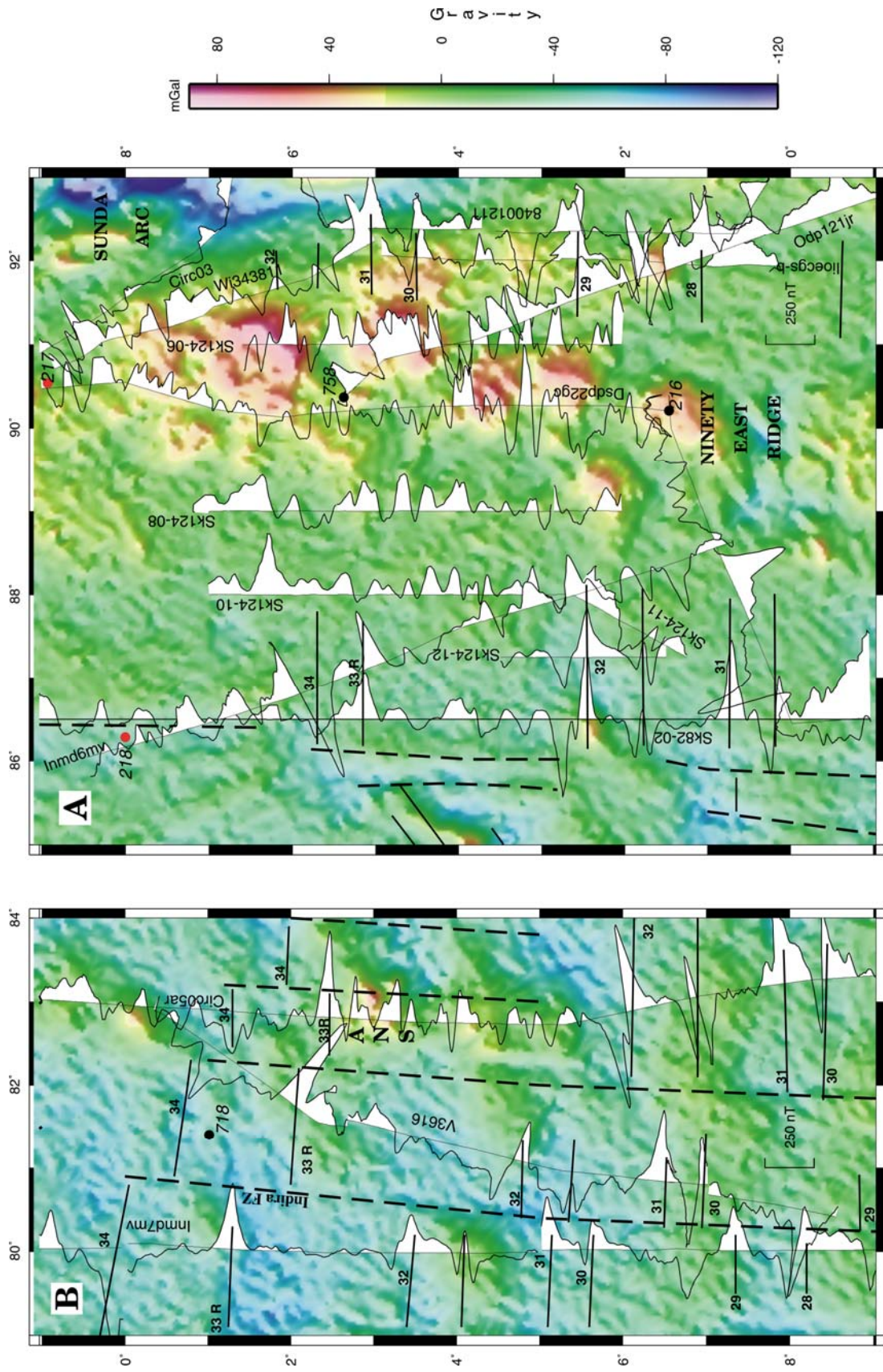
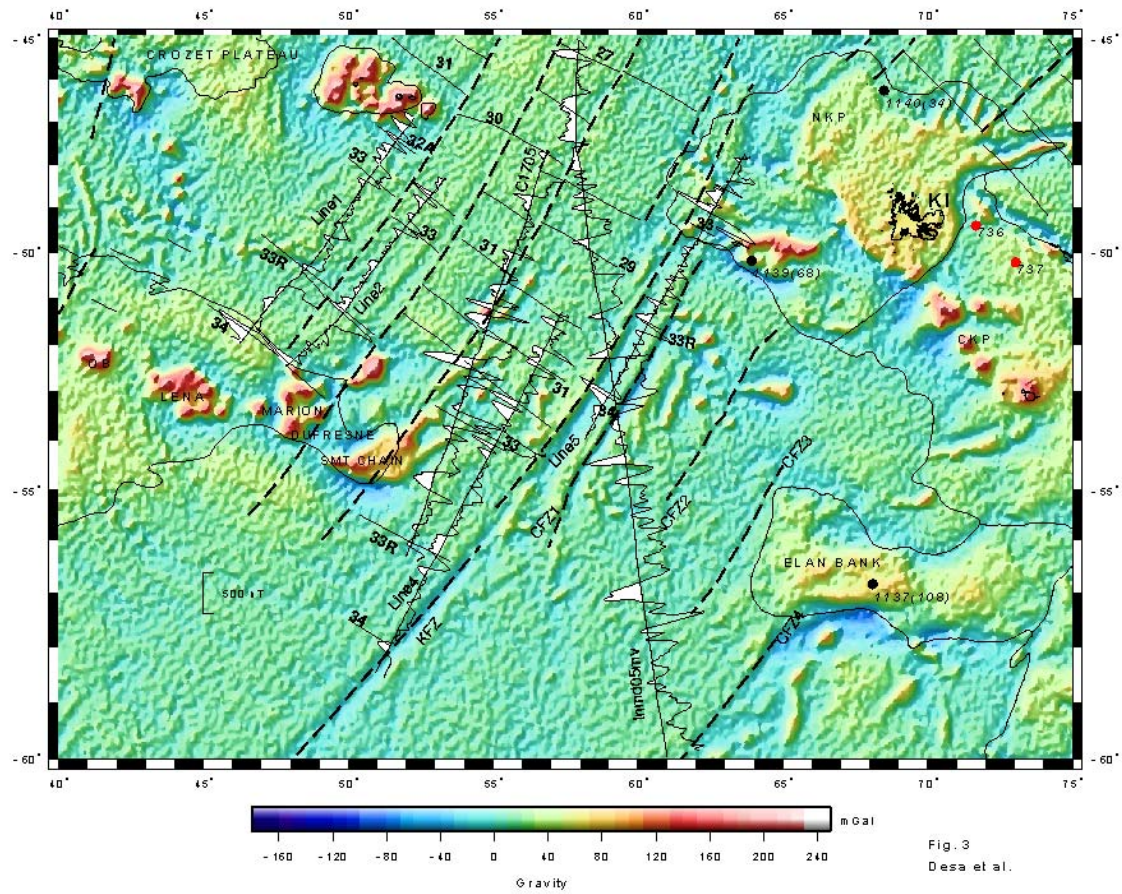


Fig. 2
Desa et al.



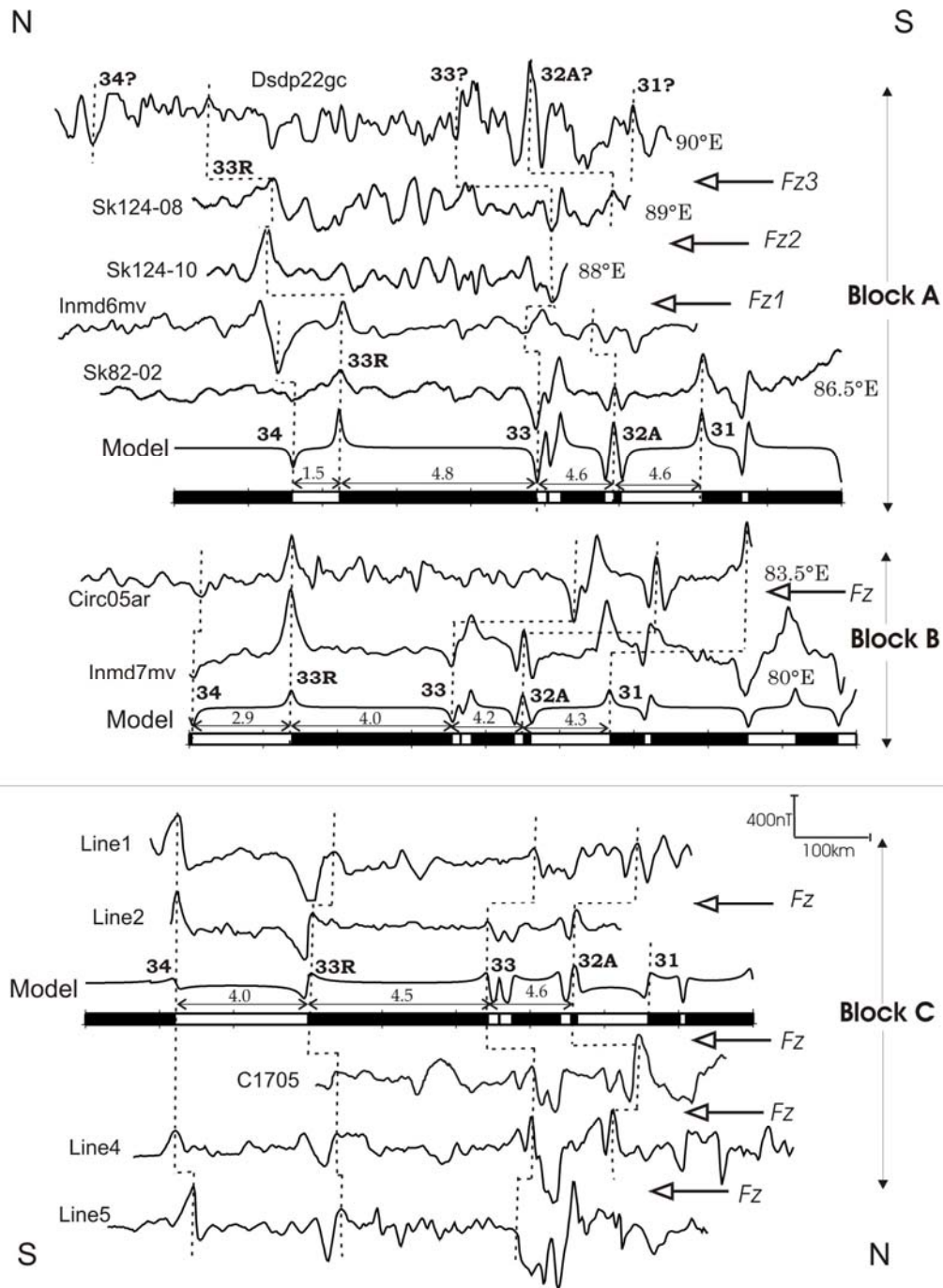


Fig. 4
Desa et al

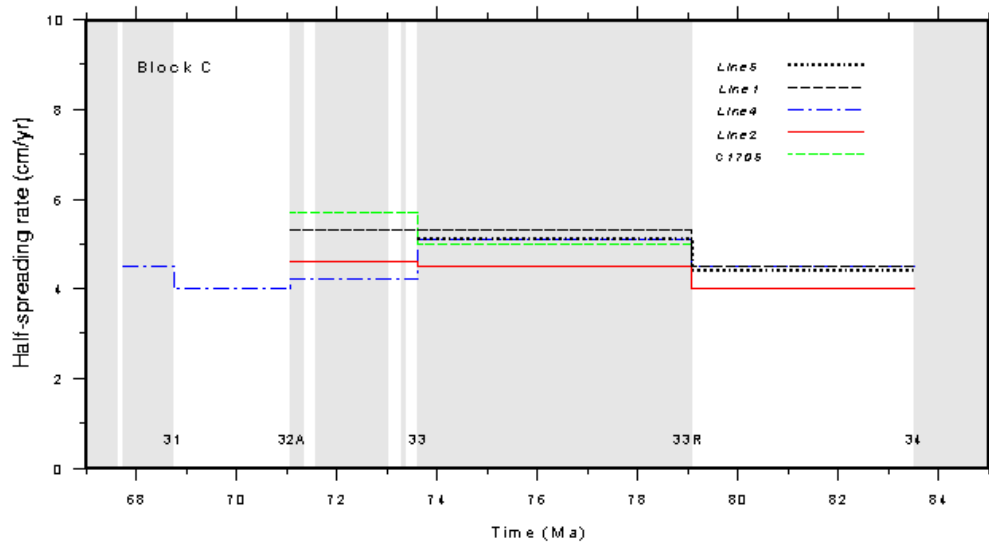
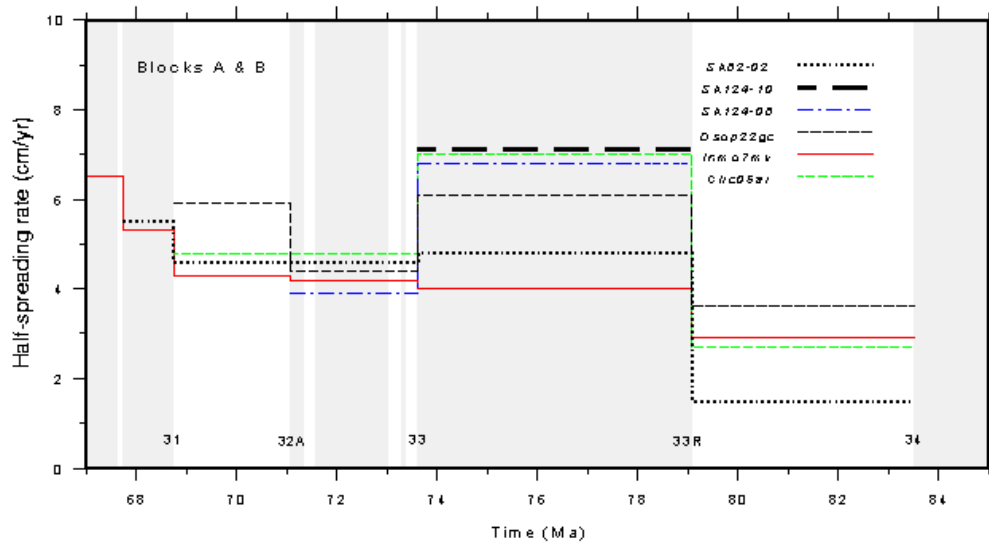


Fig. 5
Desa et al.

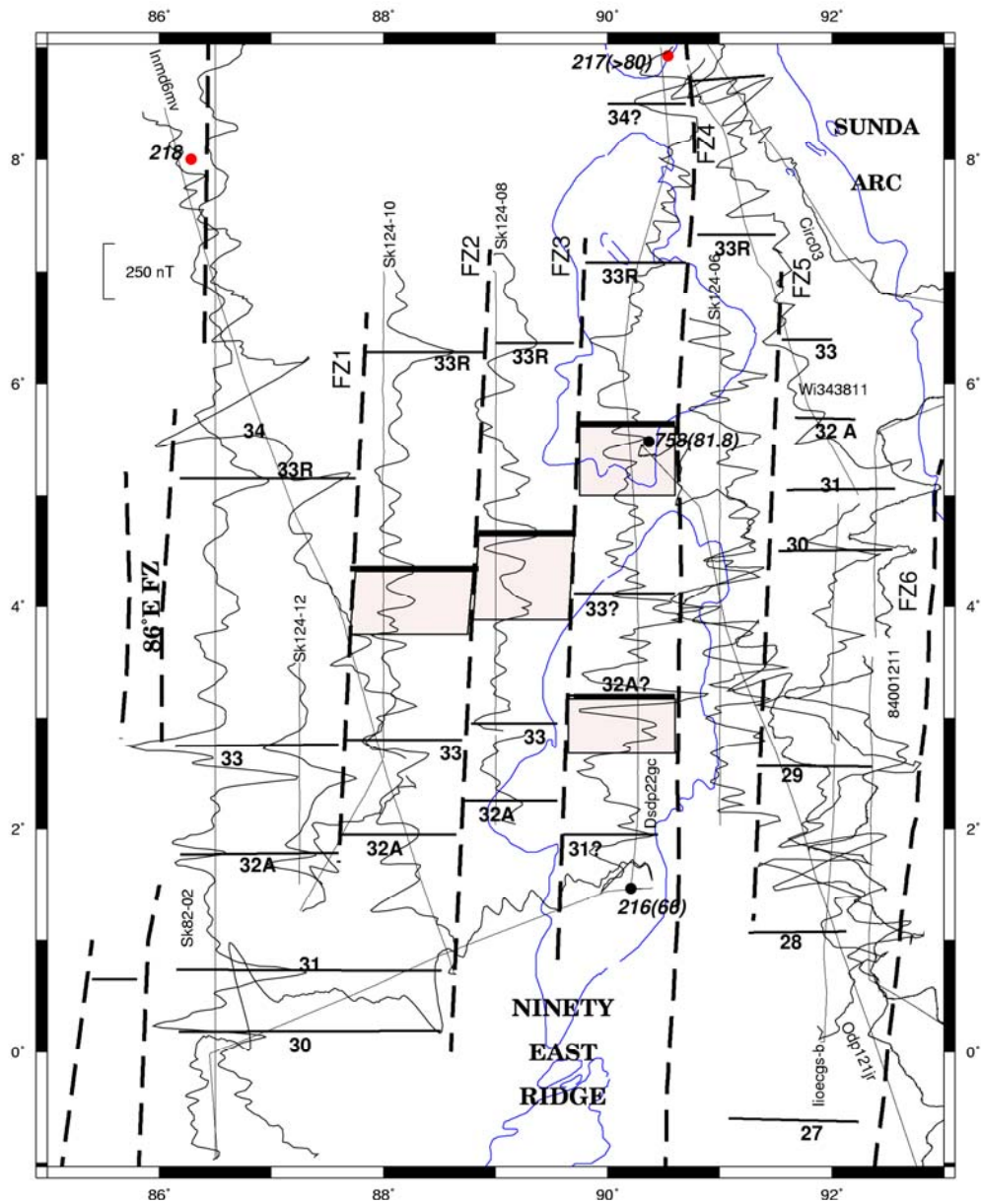


Fig. 6
Desa et al.

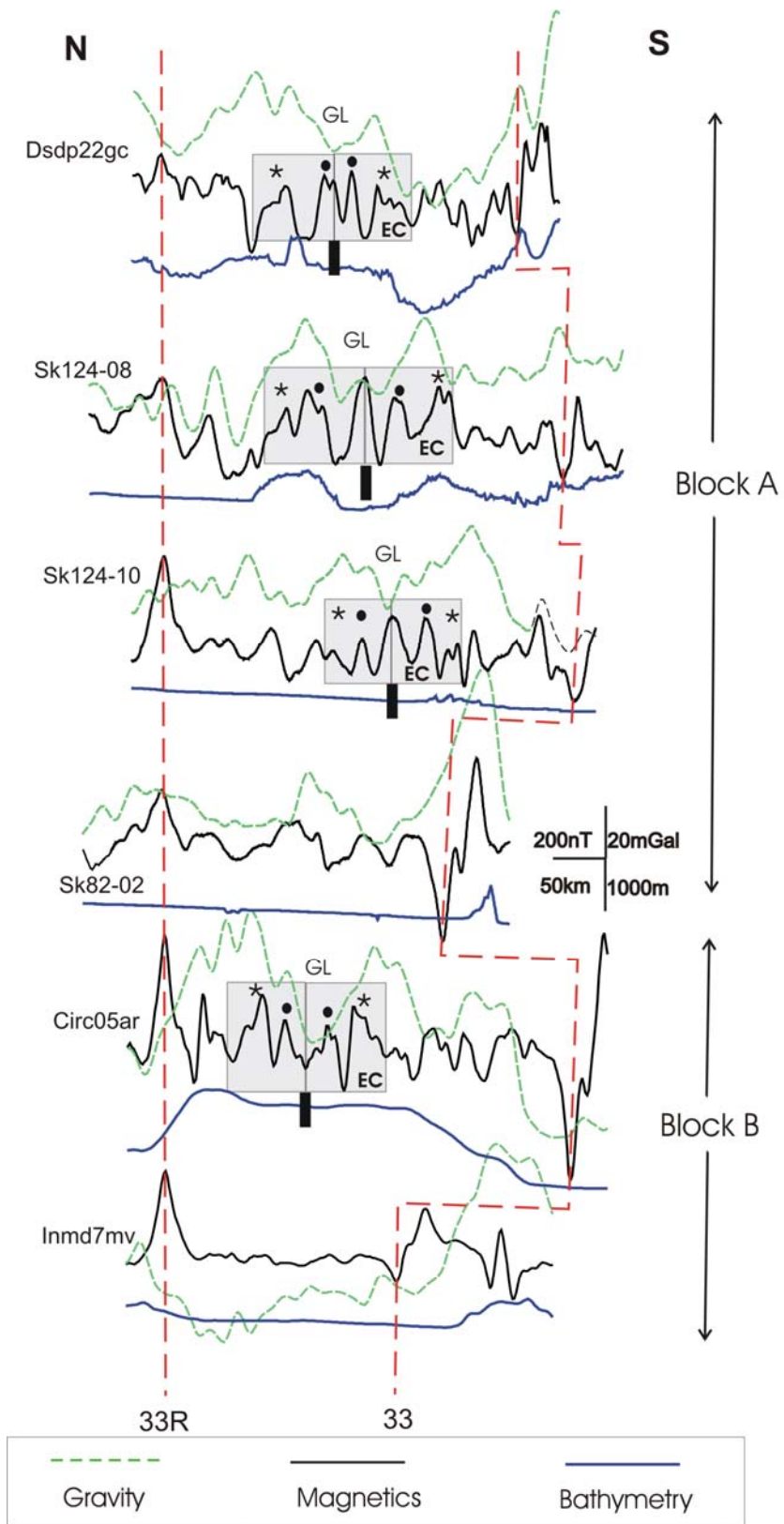


Fig. 7a
Desa et al

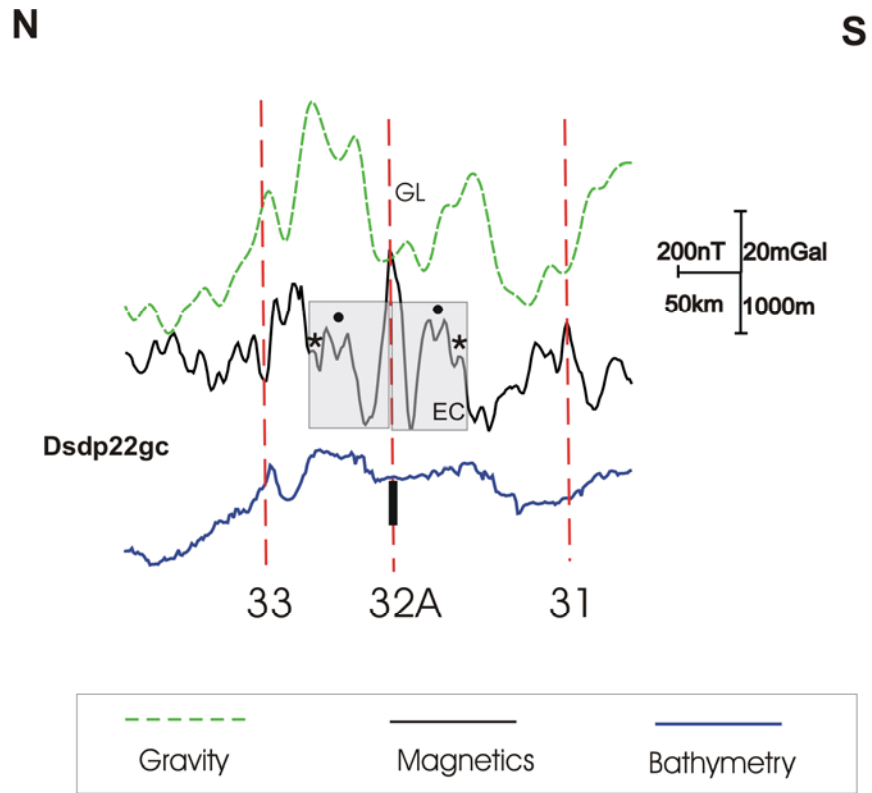


Fig. 7b
Desa et al

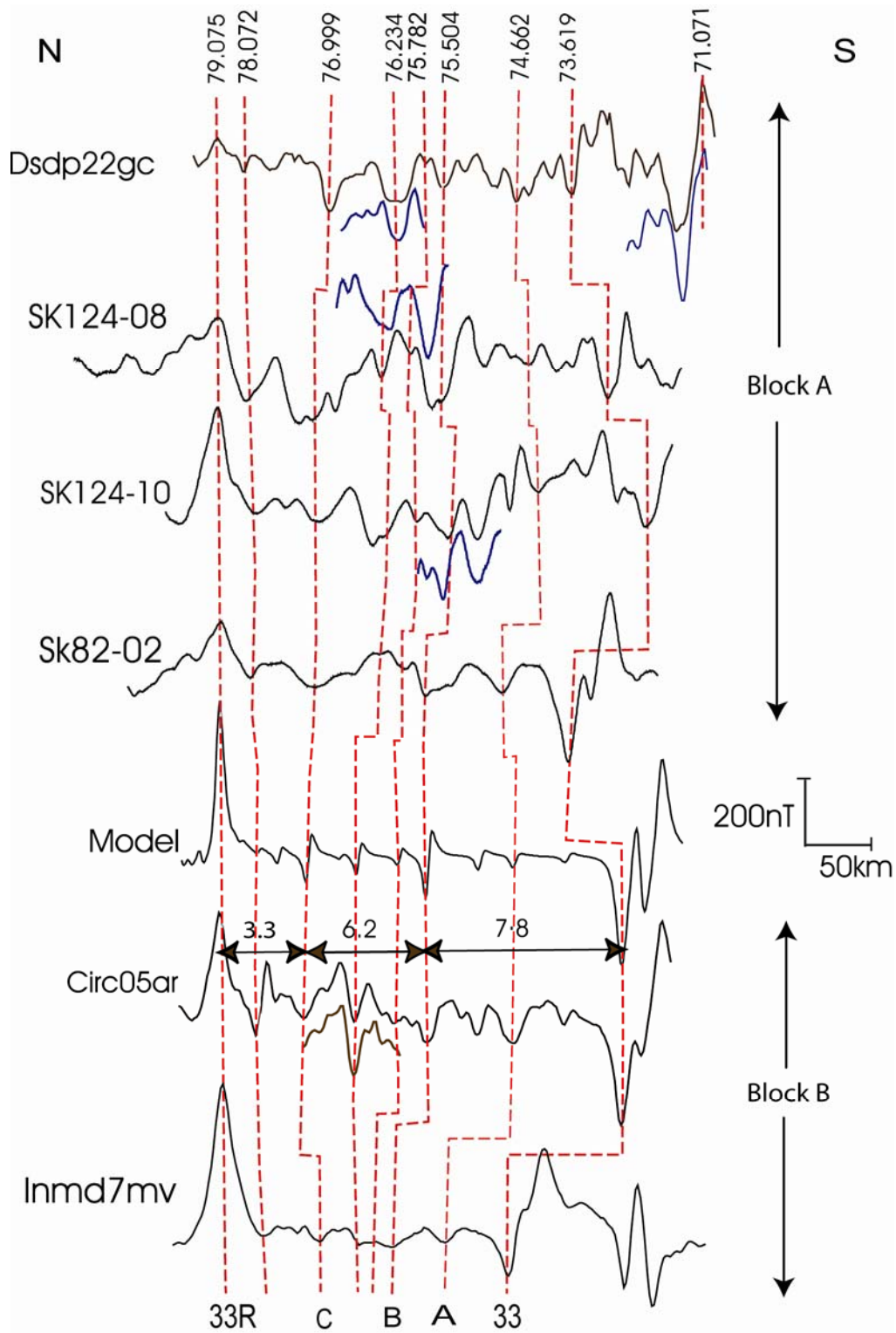


Fig. 8
Desa et al

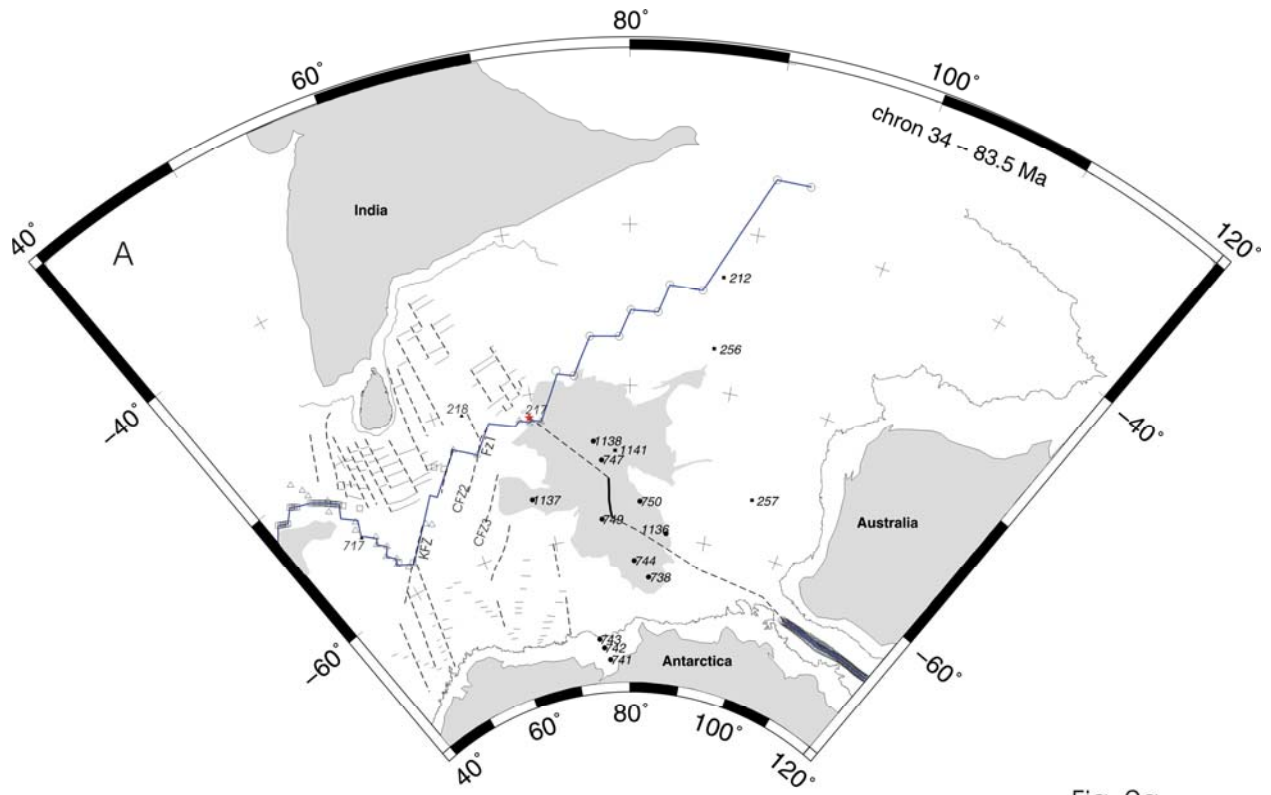
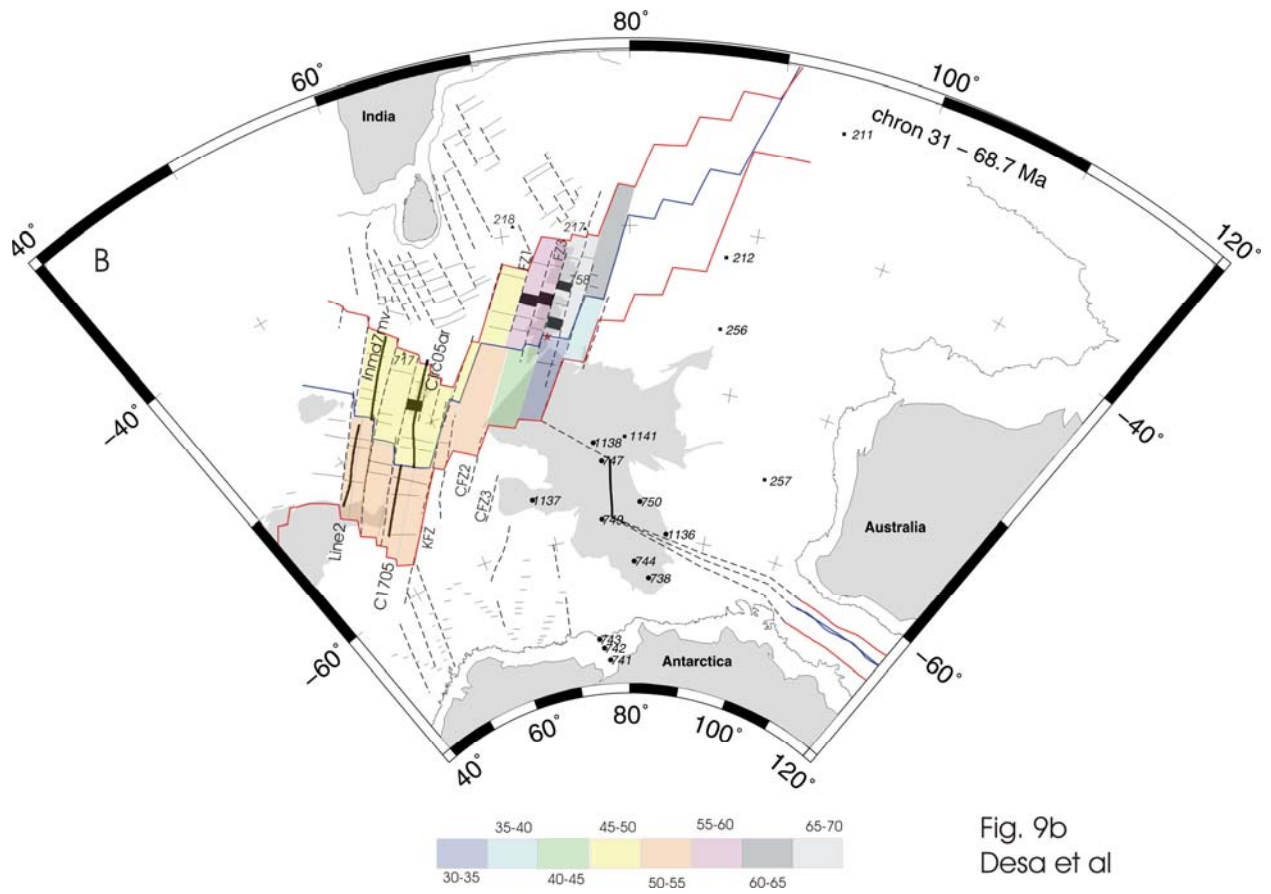


Fig. 9a
Desa et al



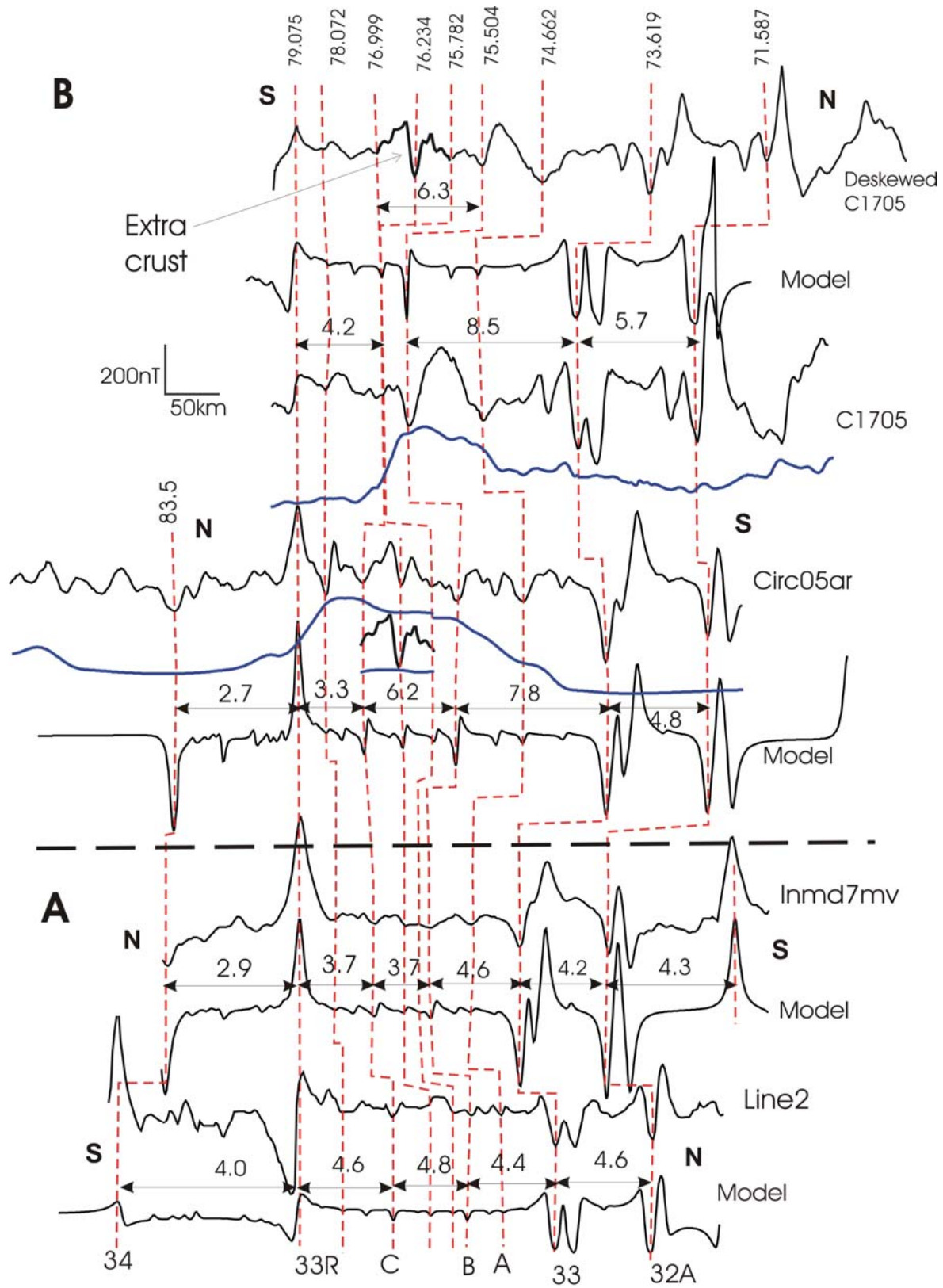


Fig 10
Desa et al